Rate sensitivity of compressive strength of columnar-grained ice

Sinha, N. K.

Publisher's version / Version de l'éditeur:

Experimental Mechanics, 21, 6, pp. 209-218, 1981-06

National Research Council Canada
Conseil national de recherches Canada

RATE SENSITIVITY OF COMPRESSIVE STRENGTH OF COLUMNAR-GRAINED ICE

by Nirmal K. Sinha

Reprinted from
Experimental Mechanics
Vol. 21, No.6, June 1981
p. 209 - 218

DBR Paper No. 1009
Division of Building Research

Price $1.00 OTTAWA NRCC 19756

Canada

SOMMAIRE

On décrit les méthodes de sélection et de préparation des éprouvettes et le détail des procédures d'essai, y compris l'examen microstructurel, que l'on applique à la mesure de la résistance à la compression uniaxiale de la glace columno-grenue. On démontre que les vitesses de déformation de l'éprouvette ne sont pas constantes pour une vitesse de déplacement transversal constante, et que, de ce fait, les résultats ne sont pas représentatifs d'une condition à vitesse de déformation constante. L'analyse met en lumière que les essais à vitesse de déplacement transversal constante correspondent plus étroitement à une condition où la vitesse d'application des contraintes est constante. Cette communication analyse aussi les déformations de rupture, les temps de rupture, le mode de défaillance et la dépendance possible des résistances sur la rigidité de l'appareillage d'essai.

Rate Sensitivity of Compressive Strength of Columnar-grained Ice

Dependence of the compressive strength of columnar-grained ice on strain rate, time, stress rate and machine stiffness is investigated for a loading condition of constant rate of cross-head displacement

by Nirmal K. Sinha

ABSTRACT—Methods of selecting and preparing specimens and details of test procedures, including those for microstructural examination, are described for the investigation of uniaxial compressive strength of columnar-grained ice. It is shown that specimen strain rates are not constant for constant cross-head-displacement rate, and that consequently the results are not representative of the constant strain-rate condition. Analysis shows that constant cross-head-displacement tests are more closely representative of the constant stress-rate condition. The paper also discusses failure strains, failure times, mode of failure and possible dependence of strength results on stiffness of the test system.

Symbols

$A, B, C, D, \alpha, \beta, \theta, \delta$ = constants
σ = stress, $MN \cdot m^{-2}$
σ_1 = unit stress = 1 $MN \cdot m^{-2}$
σ_f = upper yield or failure stress, $MN \cdot m^{-2}$
t = time, s
t_1 = unit time = 1 s
t_f = yield or failure time, s
$\dot{x}$ = constant cross-head-displacement rate, cm s^{-1}
L = specimen length, cm
ϵ = strain
ϵ_f = upper yield or failure strain (measured on sample sides in direction parallel to load axis)
ϵ_{nf} = nominal yield or failure strain $= \dot{\epsilon}_n t_f$
$\dot{\epsilon}_{af}$ = average strain rate to yield or failure, $s^{-1} = \epsilon_f / t_f$
$\dot{\epsilon}_p$ = peak strain rate (measured on sample sides), s^{-1}
$\dot{\epsilon}_n$ = nominal strain rate, $s^{-1} = \dot{x}/L$
$\dot{\epsilon}_1$ = unit strain rate, 1 s^{-1}
$\dot{\sigma}_{af}$ = average stress rate to yield or failure, $MN \cdot m^{-2}\ s^{-1} = \sigma_f / t_f$
$\dot{\sigma}_i$ = effective stress rate during most of loading, $MN \cdot m^{-2}\ s^{-1}$
E_f = failure modulus, $MN \cdot m^{-2} = \sigma_f / \epsilon_f$
E_s = effective system modulus, $MN \cdot m^{-2} = \dot{\sigma}_i / \dot{\epsilon}_n$

Introduction

One of the challenging engineering problems is that of estimating the maximum force a moving ice sheet might exert on a structure. It is analogous to the problem of the force a structure might exert in moving against a floating ice sheet, for example, in the operation of icebreaking ships. Its solution requires information on the strength and deformation of polycrystalline ice. In principle, it should be possible to design structures with sufficient strength to withstand the pressures of ice when it comes in contact with them.

The strength or yield point of a material is defined in different ways; the choice usually depends on the nature of the engineering problem. With ice, it is the maximum stress in compression that is in many situations of prime engineering concern. In this paper the maximum stress is associated with failure or yield.

A program of observation was undertaken on the uniaxial compressive creep and recovery of columnar-grained fresh-water ice, known as S-2 ice, with the load axis normal to the columns. This type of ice and stress condition is common for many field situations. The development of a rheological model, including transient creep, has been presented.[1] Many apparent inconsistencies in the results of earlier investigations of the flow law of polycrystalline ice, particularly important to engineering problems, appear to have been reconciled.[2] The present report is an extension of these investigations and examines the rate sensitivity of the uniaxial compressive strength of the same type of ice.

Information on the strength of ice is rather scattered and difficult to interpret, due mainly to lack of detailed information on experimental conditions and measurements. An additional purpose of this study was to develop systematic methods of testing and analyzing such results in the hope that this would permit more critical examination of available information and provide a better foundation for future investigations.

Preparation and Selection of Ice

A detailed description of the method of preparation and selection of inclusion-free (density = 917.7 ±0.3* kg/m^3), columnar-grained S-2 ice is available.[1] This was strictly followed in the present study with one exception:

Nirmal K. Sinha (SESA Member) is Research Officer, Geotechnical Section, Division of Building Research, National Research Council of Canada, Ottawa, Canada KIA 0R6.

Paper was presented at 1979 SESA Spring Meeting held in San Francisco, CA on May 20-25.

Original manuscript submitted: May 1979. Author notified of acceptance: May 1980. Final manuscript received: July 23, 1980.

Since the submission of Ref. 1, the method of measurement has been improved by M. Nakawo. The value given above was obtained at −9°C.

Reprinted from EXPERIMENTAL MECHANICS, Vol. 21, No. 6, 209-218, June 1981.

the choice of grain size in the cross-sectional area of the columnar grains.

It was anticipated that a large number of specimens would be required to complete the study. It takes about four weeks to prepare and grow ice from which only a few good specimens can be made. Previous experience showed that it is extremely difficult to obtain the necessary large number of specimens of the same average grain size. It was decided, as a compromise born of practical necessity, to use specimens with average grain diameter ranging from 4 to 5 mm.

Preparation of Specimens

Rectangular specimens 5 × 10 × 25 cm were prepared in a cold room at −10°C in such a way that the long direction of the grains was perpendicular to the 10 × 25-cm face. The specimens were machined to their final dimensions of 5 × 10 × 25 cm by careful milling. Surfaces were then smoothed with fine emery paper on a surface table and polished with tissue paper lightly moistened with alcohol. The transparent specimens were measured and weighed to determine average density, which was then compared with the density of a sample measured by a more accurate method. The specimens were stored in a kerosene bath inside a cold room until the tests were conducted a week or more after preparation. Immediately before each test, the end faces, 5 × 10 cm, were given a final polish to remove any imperfections that might have been introduced during storage (kerosene is known to be slightly erosive for ice stored in it for a long time).

Experimental Procedures

Compressive loads were applied to the 5 × 10 cm faces by a screw-driven test machine of 100 kN capacity (Instron, TTDM-L) with its load frame situated inside the cold room; the control panel was kept outside near a glass window. The temperature at any point in this cold room can be maintained constant for weeks and months within ±0.25°C of a required set temperature. The loading column consisted of two machined and ground steel platens (1.6 × 7.6 × 12.6 cm), one at the top and one at the bottom of the specimen, a 1.9-cm-diam steel ball and socket seat, and two 50-kN calibrated load cells (Instron and an auxiliary) in series (Fig. 1).

The Instron load cell recorded the load–time history on a strip-chart recorder kept outside the cold environment and served as a visual guide of progress of a test. The output of the other load cell was recorded by a digital data-logging system also kept outside the cold room. Simultaneous recording was made of the movement of the cross head with respect to a fixed reference point (using a direct-current linear-variable-differential transformer, DCDT), the temperature of the specimen, and the deformation in the central 3/5 of the specimen by means of a pair of strain gages (gage length = 15 cm) attached to the 10 × 25-cm faces. The strain gages and the precautions necessary in installing them have been described[1] and may be seen in Fig. 1.

For tests lasting more than a few minutes, the specimens were wrapped with clear plastic sheets[1] to prevent sublimation. A thin layer of kerosene on the exposed surfaces was found sufficient to stop any sublimation for tests of shorter duration. This protection also helped to maintain the specimen temperature and to avoid thermal gradients produced by reduction of the specimen-surface temperature due to sublimation. Tests were conducted at −10°C ±0.25°C.

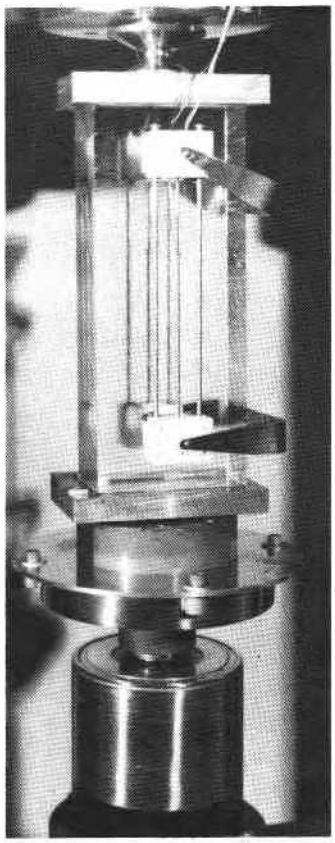

Fig. 1—Experimental arrangements inside cold room showing the ball-seat socket, the steel platens, load cells, and strain gages on specimen

During deformation columnar-grained ice has a marked tendency to develop long, narrow internal cracks parallel to the length of the columns. Their formation has a profound influence on compressive creep properties.[3] This prompted an investigation of cracking activity during the present test series and specimens were subjected to continuous visual surveillance during loading. The times for the formation of the first and a few subsequent visible cracks were marked, using manually operated electrical pulses, on the strip-chart recording-load history.

Immediately after the load reached its maximum value, depending on the cross-head rate used, the specimen was unloaded very rapidly and allowed to recover until there was no further change in strain with time. This method was used to determine the permanent and recoverable strain at or near the yield point corresponding to a given loading condition.

The number of cracks intersecting the central 10 × 15-cm area of the two 10 × 25-cm faces were then counted, using a low-power microscope. Total number of cracks in the specimen were also counted within the specified 3/5 of the specimen, provided all the cracks could be identified separately. The specimen was then sectioned in the middle plane parallel to the 10 × 25-cm faces. One of the cut surfaces was polished and the number of cracks in the section corresponding to the above-mentioned area were counted. The average crack density per unit area in the plane containing the load axis and normal to the columnar grains was then estimated using all the above data. As the specimen was unloaded immediately after yielding, crack

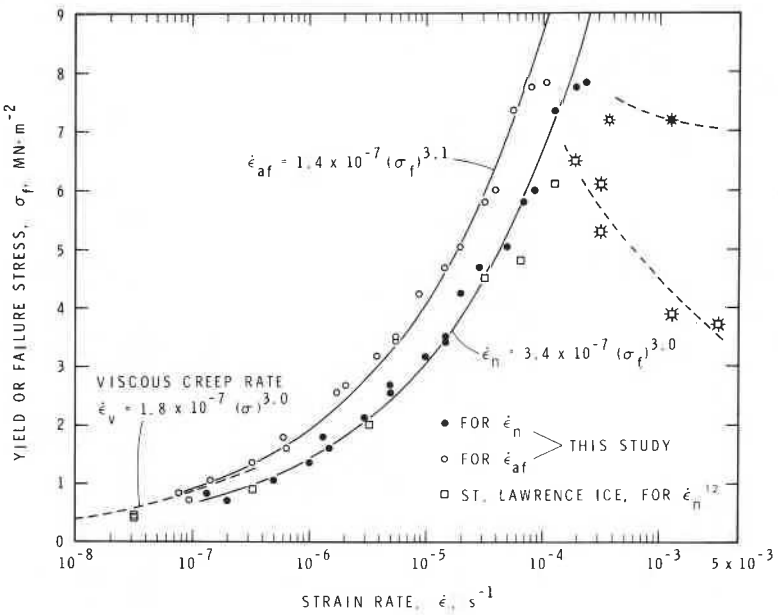

Fig. 2—Dependence of yield or failure stress on nominal strain rate, $\dot{\epsilon}_n$, and average strain rate to peak stress, $\dot{\epsilon}_{af}$, for columnar-grained ice of average grain size, 4-5 mm, at −10°C. Premature failures are marked with asterisks

density provided a measure of the structural degradation at the yield point.

A thin section (10 × 10 cm) representing the middle plane was then made from the other half of the specimen.[4] The section was photographed in transmitted light through cross-polaroids as well as in a combination of transmitted polarized light and scattered light in order to measure grain size and distribution. The latter method provided the better visual record of individual grains and the relative position of cracks. The upper surface of the thin section was then etched and replicated[4] for microstructural examination.[5]

Average grain diameter of a specimen was estimated from the average grain area determined by counting the number of grains over the entire thin-section photograph. Results for specimens having average grain diameter differing by more than the error of measurement of ±0.2 mm from the intended range discussed earlier were excluded from the present analysis and kept for future use.

Accepted Analysis

Dependence of Strength on Nominal Strain Rate

Except for the new generation of closed-loop systems, most universal test machines are designed to deliver constant rates of cross-head displacement, $\dot{x}$. The ratio of this rate to the length, L, of the specimen, for specimens of uniform cross section, will be defined as the nominal strain rate, $\dot{\epsilon}_n$. The range of $\dot{\epsilon}_n$ ($= \dot{x}/L$) to be discussed varied from 3.3×10^{-8} to 3.3×10^{-3} s^{-1}, corresponding to the cross-head rates, $\dot{x} = 8.3 \times 10^{-7}$ to 8.3×10^{-2} cm s^{-1} for the specimen length of 25 cm.

The failure response for $\dot{\epsilon}_n$ higher than 2.5×10^{-4} tended to be brittle, leading to premature cleavage type of failure. It was concluded that the tolerances between the platens and the sample end surfaces will have to be further reduced and that the geometry of the specimen itself will probably have to be changed before reliable results can be obtained for higher strain rates. For $\dot{\epsilon}_n$ less than about 5×10^{-7}, the material behaved in a viscous manner, with negligible internal-cracking activity. In the intermediate range, however, a distinct upper yield was noticed, with load decreasing rapidly after reaching a maximum value. The material exhibited an increasing number of uniformly distributed internal cracks with increase in strain rate in this range. The former behavior will be called 'viscous yield' in order to distinguish it from that showing 'upper yield'.

Experimental results are shown in Fig. 2; for the sake of clarity, the results of premature failures are purposely not shown, except for one, an example of the general trend. As the total strains at failure (described later) were small, less than 3×10^{-3}, the stresses estimated from the loads and cross-sectional areas could be considered the true stresses. The maximum stress, σ_f, was found to vary with $\dot{\epsilon}_n$, as shown in Fig. 2, according to the following dimensionally balanced empirical relation

$$\frac{\dot{\epsilon}_n}{\dot{\epsilon}_1} = A \left(\frac{\sigma_f}{\sigma_1}\right)^{\alpha} \qquad (1a)$$

where σ_1 and $\dot{\epsilon}_1$ are unit stress (MN • m^{-2}) and unit strain rate (s^{-1}), respectively. A and α are constants. Equation (1a) is given here in a form convenient for a direct comparison, to be made later, with a similar relationship commonly used to describe the dependence of viscous strain rate on stress under constant-stress-creep condition.[1,2] The constant A is interpreted here as the applied strain rate under which the strength is unity.

The results of the regressional analysis of the experimental data on the basis of eq (1a) are given in detail in

TABLE 1—REGRESSION ANALYSES FOR THE SERIES OF TESTS ON COLUMNAR-GRAINED ICE

Equation No.	Equation	Coefficient	Exponent	Correlation Coefficient
(1a)	$\frac{\dot{\epsilon}_n}{\dot{\epsilon}_1} = A \left(\frac{\sigma_f}{\sigma_1}\right)^{\alpha}$	$A = 3.37 \times 10^{-7}$ $\pm 0.34 \times 10^{-7}$	$\alpha = 3.03$ ± 0.08	0.994
(2a)	$\frac{\dot{\epsilon}_{af}}{\dot{\epsilon}_1} = B \left(\frac{\sigma_f}{\sigma_1}\right)^{\beta}$	$B = 1.39 \times 10^{-7}$ $\pm 0.15 \times 10^{-7}$	$\beta = 3.05$ ± 0.08	0.994
(3a)	$\frac{t_f}{t_1} = C \left(\frac{\sigma_f}{\sigma_1}\right)^{-\theta}$	$C = 3.35 \times 10^{3}$ $\pm 0.28 \times 10^{3}$	$\theta = 2.30$ ± 0.07	0.992
(12a)	$\frac{\dot{\sigma}_U}{\dot{\sigma}_1} = D \left(\frac{\dot{\sigma}_{af}}{\dot{\sigma}_1}\right)^{\delta}$	$D = 1.11$ ± 0.02	$\delta = 0.982$ ± 0.003	0.9999

Table 1. With $A = 3.4 \times 10^{-7}$ and $\alpha = 3.0$, given in Table 1, eq (1a) becomes

$$\frac{\dot{\epsilon}_n}{\dot{\epsilon}_1} = 3.4 \times 10^{-7} \left(\frac{\sigma_f}{\sigma_1}\right)^{3.0} \qquad (1b)$$

The above results are in general agreement with the few highly scattered data on natural S-2 ice reported by Gold and Krausz,[6] and a few on laboratory-grown ice reported by several other investigators.[7-10] The trend observed in the present investigation is similar to the characteristics reported for other types of ice.[6,8-11]

A previous set of tests[12] on naturally occurring S-2 ice from Lac St. Pierre in the St. Lawrence River (Canada) is of particular interest (Fig. 2). The tests were performed at DBR/NRC on the same test machine and using the same components in the loading column except for the auxiliary load cell. Specimens were prepared in the same way, except for the final finishing (described previously) of the end surfaces, and were identical in dimension and similar in grain size to those used in the present study. They show good agreement in the yield region and exhibit uncertainty in the results of premature failures beyond $\dot{\epsilon}_n$ greater than 1.3×10^{-4} s^{-1}.

Criticism

Specimen Strain Rate

Because strain gages[1] employing DCDT's are expensive, they were not installed initially on the specimen, in fear (subsequently proved to be wrong) of damaging them in cases when the specimen broke abruptly and violently. Initial tests were carried out with a pair of gages mounted between the top and the bottom platens. These measurements gave what might be called 'the strain at the sample ends'. The strain rate, measured in this way, was found to increase during the test until peak stress was reached under yield type of failures. Although the peak strain rate

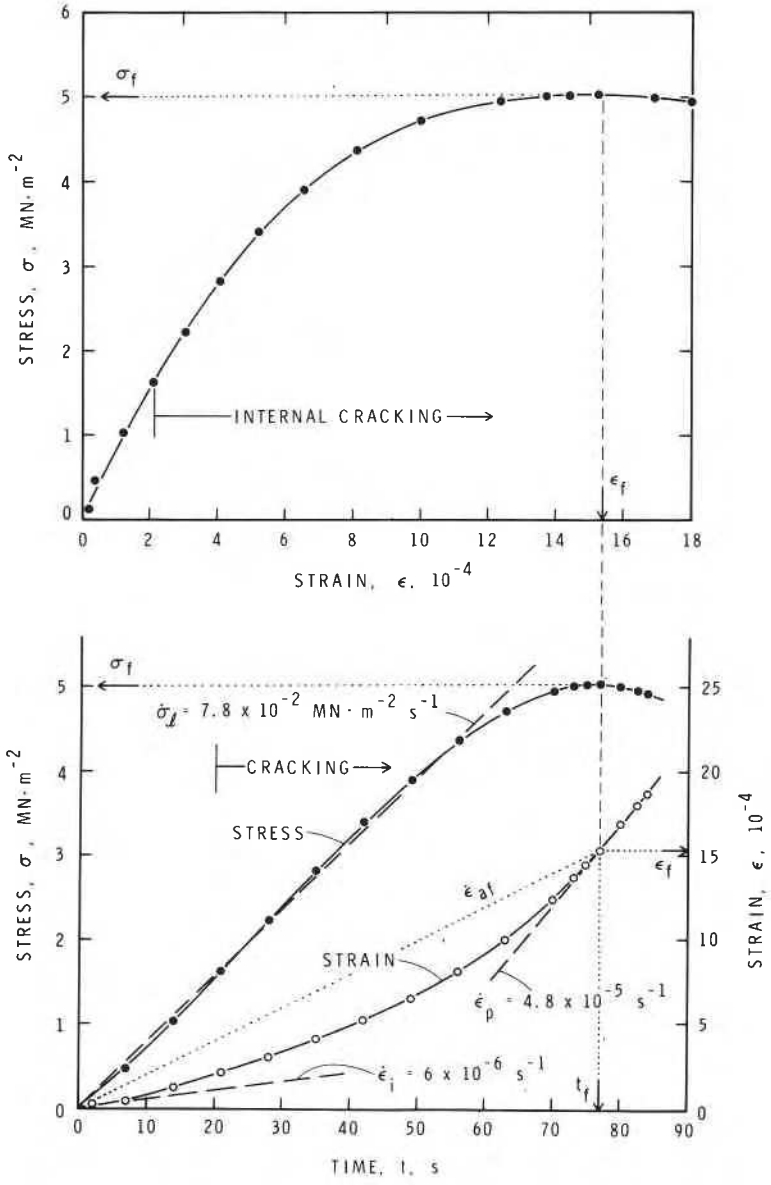

Fig. 3(a)—Stress-strain, stress-time, and strain-time results on columnar-grained ice at −10°C for a constant cross-head displacement rate of 1.25×10^{-3} cm s^{-1} or a nominal strain rate of 5×10^{-5} s^{-1}. Strain shown was the average value measured by two gages mounted on the specimen

was close to the nominal strain rate, the strain rate was very low in the beginning. Since the yield strains were very small, in the range of 0.1 percent in these tests, bulging of the specimen was not considered the main problem. In addition, bulging could not occur right at the beginning of the tests. Moreover, if bulging was a problem, then why did the specimen strain rate approach the corresponding nominal strain rate as the test progressed? The machine was, therefore, blamed for not maintaining a constant speed and a decision was made to examine the cross-head rate. Its rate of movement was measured during loading with respect to a fixed reference point. When the cross-head rate was found to be constant and equal to the set rate, then the unexpected behavior was ascribed to the end effects. The strain gages were then mounted on the 10 × 25 faces of the specimen (Fig. 1) so that the ascribed unknown end effects might be eliminated. However, the deformation rate of the sample sides (Fig. 3a) also showed variations during a test, similar to those observed in the previous tests. For confirmation, tests were then performed during which simultaneous recordings were made on the strain at the sample sides and the strain at the sample ends, the cross-head rate and a few other measurements related to the response of other components of the test system. An example of such a test result is shown in Fig. 3(b) which shows the stress and strain histories during loading as well as during recovery. The example shows that the two sets of strain measurements during loading were close to each other within experimental uncertainties, but both were far from what would have been expected if strain rate was constant at the nominal rate of 5×10^{-6} s^{-1}, corresponding to the measured constant cross-head rate of 1.25×10^{-4} cm s^{-1}. Since imperfections in the end-surface preparations of the samples were liable to introduce uncertainties in the measurements of the strain at the sample ends, it was decided to adopt the side-strain measurements as the standard procedure.

This discussion shows that the strain rate in the specimens monotonously increased with time in spite of the observed constancy in cross-head-displacement rates and approached the nominal strain rate only after reaching maximum stress. The initial strain rates were about an order of magnitude less than the subsequent maximum strain rate. The peak strain rate in the specimen, $\dot{\epsilon}_p$, estimated from a narrow range of strain-time data near yield point or after maximum stress was reached (see Fig. 3) is compared with $\dot{\epsilon}_n$ in Fig. 4. In spite of the possible large error in the estimation of $\dot{\epsilon}_p$, the equivalency between $\dot{\epsilon}_p$ and $\dot{\epsilon}_n$ is beyond question, as may be seen from the line $\dot{\epsilon}_p = \dot{\epsilon}_n$. This indicates that the testing machine was able to impose the specified deformation rate on the specimen only when the specimen offered no more increase in resistance with further increase in deformation. The use of $\dot{\epsilon}_n$ as an independent variable can therefore be justified, and the systematic variation of σ_f with it supports this. The results, however, cannot be construed as constant strain rate, although this is customarily assumed.[6-11, 13]

The occurrence of premature failure is often referred to in ice literature as 'ductile to brittle transition'. As such failures occur anywhere along the strain–time path, the strain rate in the specimen at the moment of failure can be significantly lower than the corresponding $\dot{\epsilon}_n$. This behavior has never been recognized in glaciological literature and premature failures are usually plotted as a function of $\dot{\epsilon}_n$, as shown in Fig. 2. One example from the present series is shown in Fig. 4, corresponding to the example used in Fig. 2. In this case, the strain rate at failure was estimated to be only about 35 percent of $\dot{\epsilon}_n$. It seems that the ratio of specimen strain rate at failure to $\dot{\epsilon}_n$ could be used as a measure of the 'degree of maturity' in this type of failure.

The quality of the specimen preparation could control how early premature failure occurs at higher $\dot{\epsilon}_n$ and, thereby, influence the outcome of strength results. This is evident in the trends, shown by the broken lines in Fig. 2, of the present series and that of the St. Lawrence River ice. Experimental evidence of this observation was seen and strongly emphasized by Hawks and Mellor[11] in

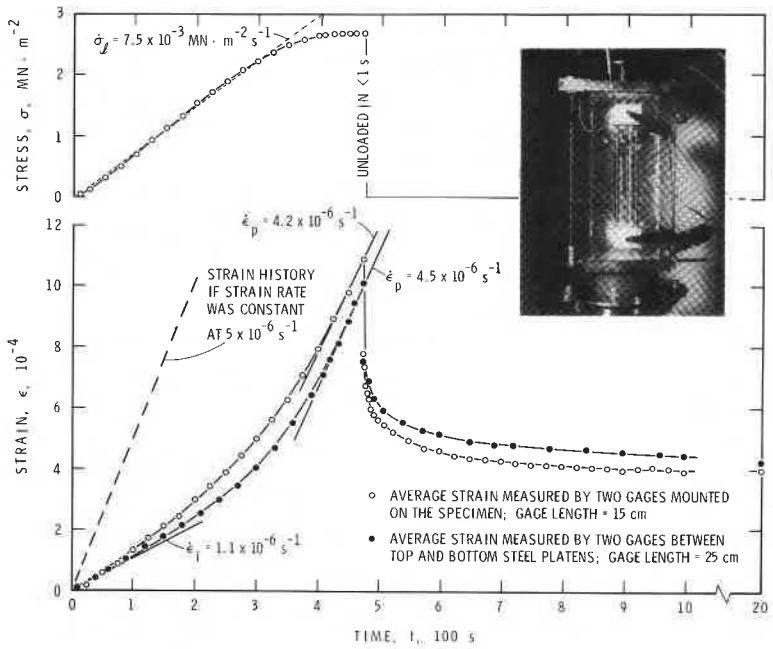

Fig. 3(b)—Stress and strain history of columnar-grained ice at −10°C subjected to a constant cross-head displacement rate of 1.25×10^{-4} cm s^{-1} or a nominal strain rate of 5×10^{-6} s^{-1} during loading. Details on strain measurements are given in the legend and the insert shows the experimental setup

an investigation on granular ice.

Average Strain Rate to Failure

A better but still far from satisfactory representation of strain history might be obtained by considering the average strain rate to yield or failure, $\dot{\epsilon}_{af}$, $(= \epsilon_f/t_f)$ determined from strain at peak stress, ϵ_f, and failure time t_f. The strain path in this presentation is equivalent to the line joining the origin and the yield point on the strain-time plot, as can be appreciated from Fig. 3.

Strength was again observed to vary systematically with $\dot{\epsilon}_{af}$ except, as before, for premature failures (Fig. 2). The results are described by the following relation

$$\frac{\dot{\epsilon}_{af}}{\dot{\epsilon}_1} = B\left(\frac{\sigma_f}{\sigma_1}\right)^{\beta} \tag{2a}$$

where B and β are constants. Results of regressional analysis of the experimental data gave $B = 1.4 \times 10^{-7}$ and $\beta = 3.1$ with a correlation coefficient of 0.994 (see Table 1 for details). With these values of B and β, eq (2a) can be written as

$$\frac{\dot{\epsilon}_{af}}{\dot{\epsilon}_1} = 1.4 \times 10^{-7}\left(\frac{\sigma_f}{\sigma_1}\right)^{3.1} \tag{2b}$$

Table 1 shows that the stress exponents α and β are equal to each other within the reported scatter. The difference between the coefficients A and B are, however, significant. This indicates that the same yield strength would occur at different strain rates depending on the way the strain rate for a given test is calculated. This raises the question: what would the strength be for a truly constant strain rate? It should be pointed out here that eq (2b) is remarkably close to the relation describing the dependence of viscous flow of ice on stress in creep proposed by this author[1,2] and illustrated in Fig. 2.

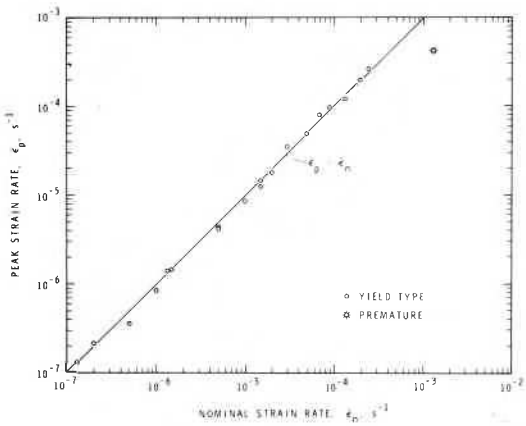

Fig. 4—Comparison of the nominal strain rate and the corresponding peak strain rate measured with a pair of gages mounted on the specimen

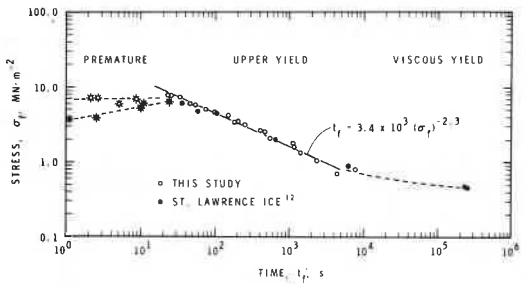

Fig. 5—Dependence of yield or failure time on yield or failure stress. Premature failures are marked with asterisks

Reinterpretation

Failure Time

Strength-measuring systems are invariably equipped to record maximum load and many, like the present one, can record the load-time history. Thus information on failure time is or can be made available. It would then be natural to examine the dependence of failure time, t_f, on the imposed loading condition. Previous discussions, however, indicated the uncertainty in the quantification of the loading condition. It was, therefore, decided to examine the inter-relationship between t_f and σ_f. Once this was determined for a system the dependence of t_f on $\dot{\epsilon}_n$ or $\dot{\epsilon}_{af}$ can be formulated if required. Figure 5 is a plot of the failure stress and the time, t_f, taken to reach it. There is a strong relation between σ_f and t_f for tests exhibiting upper yield, expressed as

$$\frac{t_f}{t_1} = C\left(\frac{\sigma_f}{\sigma_1}\right)^{-\theta} \tag{3a}$$

where C and θ are constants and t_1 is unit time (s). Results of regressional analysis of the experimental data gave $C = 3.4 \times 10^3$ and $\theta = 2.3$ with a correlation coefficient of 0.992 (see Table 1 for details). With these values of C and θ, eq (3a) can be written as

$$\frac{t_f}{t_1} = 3.4 \times 10^3\left(\frac{\sigma_f}{\sigma_1}\right)^{-2.3} \tag{3b}$$

As the stress did not show during the test a reversal point for low rates of loading, the estimation of 'time of yield' was subjective for viscous yields. Thus there was a broad, but smooth, transition from yield in pure viscous flow to yield by a combination of viscous flow and internal cracking. The question of determining the time to reach maximum stress and the corresponding strain were thought to be equivalent to the question of ascertaining the time and the strain to reach steady-state in constant stress creep tests. The time aspect of the latter subject has been discussed at length elsewhere[2] on the basis of the rheological model proposed earlier.[1]

Stress and Strain at Failure

Failure strain, ϵ_f, is related to the average strain rate to peak stress, $\dot{\epsilon}_{af}$, as defined earlier, by

$$\epsilon_f = \frac{\dot{\epsilon}_{af}}{\dot{\epsilon}_1} \times \frac{t_f}{t_1} \tag{4}$$

Substituting $\dot{\epsilon}_{af}/\dot{\epsilon}_1$ and t_f/t_1, respectively, from eqs (2a) and (3a) in eq (4) gives

$$\epsilon_f = BC\left(\frac{\sigma_f}{\sigma_1}\right)^{\beta-\theta} \tag{5a}$$

which reduces, on substitution of the values of B, C, β and θ from Table 1, to

$$\epsilon_f = 4.7 \times 10^{-4} \left(\frac{\sigma_f}{\sigma_1}\right)^{0.75} \quad (5b)$$

Equation (5b) is compared with the experimental data in Fig. 6.

In eq (4), substituting $\dot{\epsilon}_n/\dot{\epsilon}_1$ from eq (1a) for $\dot{\epsilon}_{af}/\dot{\epsilon}_1$ and using eq (3a) for t_f/t_1, gives

$$\epsilon_{nf} = AC \left(\frac{\sigma_f}{\sigma_1}\right)^{\alpha-\theta} \quad (6a)$$

which reduces, on substitution of the values of A, C, α and θ from Table 1, to

$$\epsilon_{nf} = 1.1 \times 10^{-3} \left(\frac{\sigma_f}{\sigma_1}\right)^{0.73} \quad (6b)$$

where ϵ_{nf} is what might be called 'nominal yield strain'. Equation (6b) greatly overestimates the strain at yield. This deviation is caused primarily because of the underlying assumption of constant strain rate for $\dot{\epsilon}_n$ in deriving eqs (6a) and (6b). Thus, drawing the stress–strain curve on the basis of stress–time data by replacing time with strain, assuming a constant strain rate equal to $\dot{\epsilon}_n$, could lead to erroneous results although this is frequently practiced.

Combination of eqs (5a) and (1a) results in

$$\epsilon_f = BCA^{-\frac{\beta-\theta}{\alpha}} \left(\frac{\dot{\epsilon}_n}{\dot{\epsilon}_1}\right)^{\frac{\beta-\theta}{\alpha}} = 1.9 \times 10^{-2} \left(\frac{\dot{\epsilon}_n}{\dot{\epsilon}_1}\right)^{0.25} \quad (7)$$

Combination of eqs (5a) and (2a) gives

$$\epsilon_f = B^{\frac{\theta}{\beta}} C \left(\frac{\dot{\epsilon}_{af}}{\dot{\epsilon}_1}\right)^{\frac{\beta-\theta}{\beta}} = 2.3 \times 10^{-2} \left(\frac{\dot{\epsilon}_{af}}{\dot{\epsilon}_1}\right)^{0.25} \quad (8)$$

Equations (7) and (8) relate failure strains with the corresponding nominal and average strain rates, respectively. These relations are useful in examining previous data, but will not be discussed further in this paper.

Average Stress Rate to Failure

An alternative method of analysis would be to consider the stress rates during loading. The average stress rate to failure, $\dot{\sigma}_{af}$, $(= \sigma_f/t_f)$ is given by

$$\frac{\dot{\sigma}_{af}}{\dot{\sigma}_1} = \frac{\sigma_f}{\sigma_1} \Big/ \frac{t_f}{t_1} \quad (9)$$

where $\dot{\sigma}_1$ is the unit stress rate ($MN \cdot m^{-2}\ s^{-1}$). Substitution of t_f/t_1 from eq (3a) in eq (9) gives

$$\frac{\dot{\sigma}_{af}}{\dot{\sigma}_1} = C^{-1} \left(\frac{\sigma_f}{\sigma_1}\right)^{1+\theta} \quad (10a)$$

which, on substitution of the values of C and θ from Table 1, gives

$$\frac{\dot{\sigma}_{af}}{\dot{\sigma}_1} = 3.0 \times 10^{-4} \left(\frac{\sigma_f}{\sigma_1}\right)^{3.3} \quad (10b)$$

Equation (10) should be applicable to cases exhibiting upper yield only (Fig. 7). If σ_f/σ_1 from eq (3a) is substituted in eq (9), then

$$\frac{t_f}{t_1} = C^{\frac{1}{\theta+1}} \left(\frac{\dot{\sigma}_{af}}{\dot{\sigma}_1}\right)^{-\frac{\theta}{\theta+1}} \quad (11a)$$

which, using Table 1, reduces to

$$\frac{t_f}{t_1} = 11.7 \left(\frac{\dot{\sigma}_{af}}{\dot{\sigma}_1}\right)^{-0.70} \quad (11b)$$

Loading Stress Rate

The increase in stress with time was almost linear for most of the loading time. This is shown in Fig. 3 by the line labelled $\dot{\sigma}_l$. The stress rate, $\dot{\sigma}_l$, is not a fully satisfactory description of the loading condition, but it is more representative than $\dot{\sigma}_{af}$ for about 90 to 95 percent of the maximum stress for all the tests exhibiting yield. Although there is room for improvement, the present test series can be considered more representative of constant stress rate than of constant strain rate.

It may be seen in Fig. 3 that $\dot{\sigma}_l$ is greater than $\dot{\sigma}_{af}$. Both quantities, however, were found to be related in the intermediate rates of loading, as shown in Fig. 8, giving

$$\frac{\dot{\sigma}_l}{\dot{\sigma}_1} = D \left(\frac{\dot{\sigma}_{af}}{\dot{\sigma}_1}\right)^{\delta} \quad (12a)$$

where D and δ are constants. Regressional analysis of the experimental data gave $D = 1.1$ and $\delta = 0.98$ with a correlation coefficient of 0.9999 (see Table 1 for details). With these values of D and δ, eq (12a) gives

$$\frac{\dot{\sigma}_l}{\dot{\sigma}_1} = 1.1 \left(\frac{\dot{\sigma}_{af}}{\dot{\sigma}_1}\right)^{0.98} \quad (12b)$$

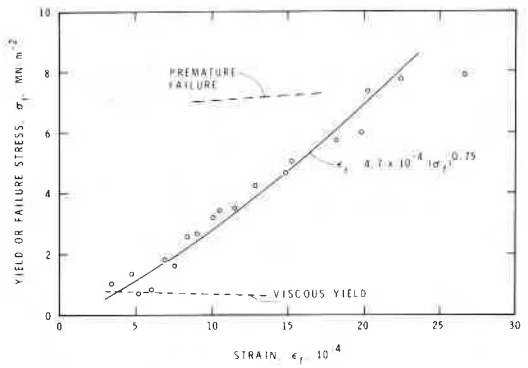

Fig. 6—Dependence of strain on stress at yield or failure. Strains shown were the average values measured by two gages mounted on the specimen

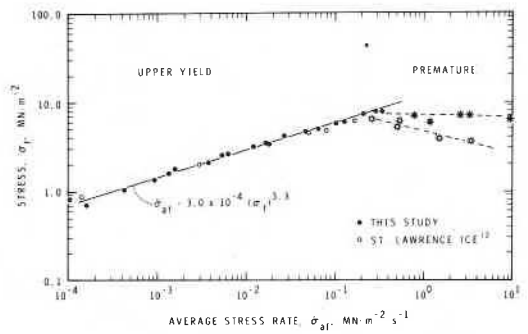

Fig. 7—Dependence of yield or failure stress on average stress rate to yield or failure. Premature failures are marked with asterisks

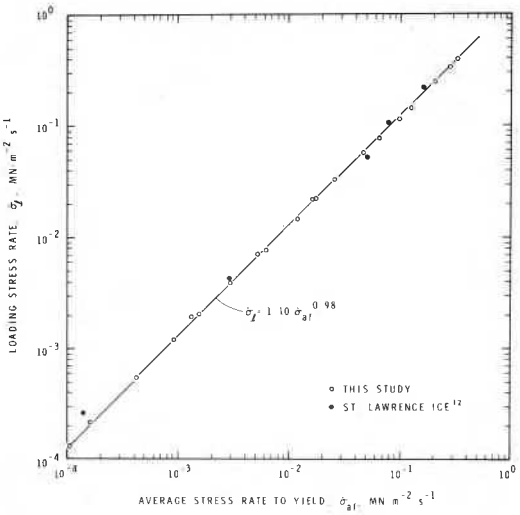

Fig. 8—Interdependence of average stress rate to yield and stress rate during loading

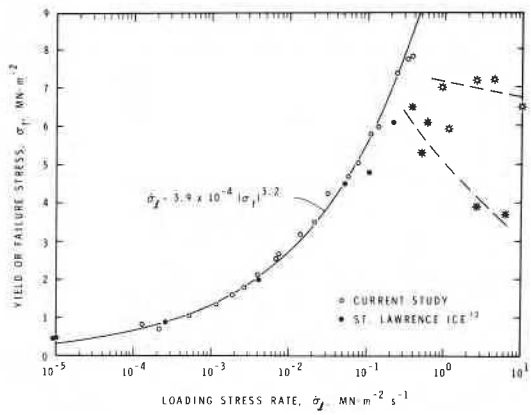

Fig. 9—Dependence of yield or failure stress on stress rate during loading. Note trends of premature failures, marked with asterisks, in the two series of tests

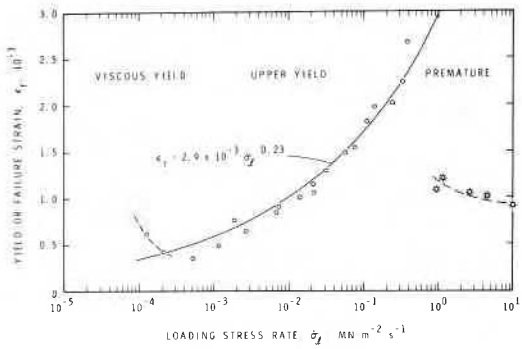

Fig. 10—Dependence of strain at yield or failure on stress rate during loading

Figure 8 also includes data points from tests on river ice.[12]

Substituting $\dot{\sigma}_{af}/\dot{\sigma}_1$ from eq (10a) in eq (12a),

$$\frac{\dot{\sigma}_f}{\dot{\sigma}_1} = C^{-\delta} D \left(\frac{\sigma_f}{\sigma_1}\right)^{\delta(1+\theta)} \tag{13a}$$

which reduces to, on substitution of the values of the constants from Table 1,

$$\frac{\dot{\sigma}_f}{\dot{\sigma}_1} = 3.9 \times 10^{-4} \left(\frac{\sigma_f}{\sigma_1}\right)^{3.2} \tag{13b}$$

Experimental results are compared with eq (13b) in Fig. 9.

Stress Rate and Failure Time

A major obstacle in using $\dot{\sigma}_f$ is that the actual failure time, as may be seen from Fig. 3, is greater than $\sigma_f/\dot{\sigma}_f$. This is a dilemma and cannot be avoided under the present circumstances. It raises the question: what would the strength be if stress rate were maintained constant until failure? The relation of t_f and σ_f can, however, be obtained from eqs (11a) and (12a), giving

$$\frac{t_f}{t_1} = C^{\frac{1}{\theta+1}} D^{\frac{\theta}{\delta(\theta+1)}} \left(\frac{\dot{\sigma}_f}{\dot{\sigma}_1}\right)^{-\frac{\theta}{\delta(\theta+1)}} \tag{14a}$$

which, using Table 1, reduces to

$$\frac{t_f}{t_1} = 12.6 \left(\frac{\dot{\sigma}_f}{\dot{\sigma}_1}\right)^{-0.71} \tag{14b}$$

Stress Rate and Failure Strain

The dependence of ϵ_f on $\dot{\sigma}_{af}$ can be obtained from eqs (5a) and (10a), giving

$$\epsilon_f = BC^{\frac{1+\beta}{1+\theta}} \left(\frac{\dot{\sigma}_{af}}{\dot{\sigma}_1}\right)^{\frac{\beta-\theta}{1+\theta}} \tag{15a}$$

which reduces to

$$\epsilon_f = 2.95 \times 10^{-3} \left(\frac{\dot{\sigma}_{af}}{\dot{\sigma}_1}\right)^{0.23} \tag{15b}$$

Equations (12a) and (15a) then give the dependence of ϵ_f on $\dot{\sigma}_f$

$$\epsilon_f = BC^{\frac{1+\beta}{1+\theta}} D^{-\frac{\beta-\theta}{\delta(1+\theta)}} \left(\frac{\dot{\sigma}_f}{\dot{\sigma}_1}\right)^{\frac{\beta-\theta}{\delta(1+\theta)}} \tag{16a}$$

which reduces, using Table 1, to

$$\epsilon_f = 2.9 \times 10^{-3} \left(\frac{\dot{\sigma}_f}{\dot{\sigma}_1}\right)^{0.23} \tag{16b}$$

Both eqs (15b) and (16b) describe the experimental results satisfactorily. As they are interrelated, only one graphical comparison (Fig. 10) is considered sufficient to illustrate their applicability. Note the stress-rate dependence of the strain to viscous yield or premature failure in Fig. 10. The trend shown for abrupt failures indicates a decrease in strain with increasing load rate, indicative of the increase in degree of prematurity.

Crack Formation

Although detailed discussion of this subject will be presented elsewhere, a few pertinent points are worth mentioning. Crack density increased rapidly from 0.007 cm^{-2} to about 8 cm^{-2} for an increase in yield stress from 0.7 MN • m^{-2} to about 7 MN • m^{-2}. Distinct upper yields also occurred when maximum stress exceeded about 1.0

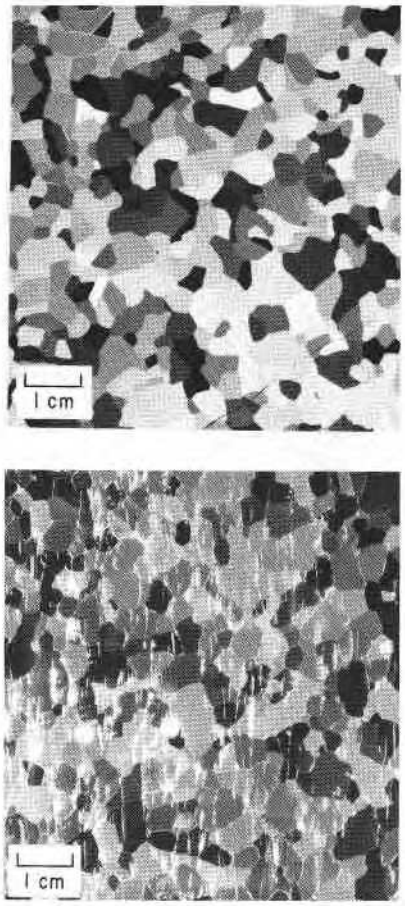

Fig. 11—Mid-plane thin-section photographs showing variation in the structure for yield stresses of 0.7 MN•m^{-2} (top) and 6.0 MN•m^{-2} (bottom). Compression axis in vertical direction. Note predominant orientation of cracks in bottom photograph

MN•m^{-2}. An increase in loading rate thus gradually changed the mode of failure from yield without cracks to total collapse of the structure as a result of internal cracks (Fig. 11). Premature failures, on the other hand, were characterized by the absence of a significant number of internal cracks in the broken segments that failed early.

Gold[3] reported the formation of cracks in columnar-grained ice in uniaxial compressive creep when stress exceeded about 0.6 MN•m^{-2}. He also noted that structural deterioration due to crack formation caused the primary stage of creep to change directly to the accelerating stage when stress exceeded about 1.2 MN•m^{-2}. Such observations seem to be analogous to the strength level above which the cracks formed and the stress above which well-defined yield points developed.

Machine Stiffness

No doubt, deformation history influences the cracking activities and strength properties of ice. In turn, deformation history must be influenced by the test conditions. It is desirable, therefore, to examine the response, particularly the stiffness, of the test system used and its possible effects on the results obtained.

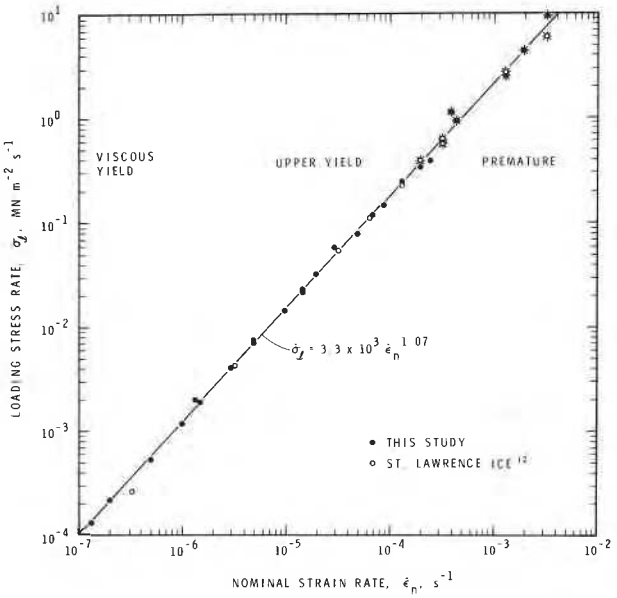

Fig. 12—Dependence of stress rate during loading on nominal strain rate. Premature failures are marked with asterisks

The stiffness of a test system depends on the rigidity of all components and their junctions as well as the material properties of the specimen and its geometry. It is difficult to predict the response of the total system when the material in question is nonlinear viscoelastic. Several methods of analysis were investigated for the system. One of the simplest measures of its effective stiffness was found by relating $\dot{\epsilon}_n$ and the resultant $\dot{\sigma}_f$. The choice was prompted by the observed constancy in the cross-head-displacement rate and the nearly constant stress rate during a test. Moreover, it was useful in examining previous data.

Substitution of σ_f/σ_1 from eq (1a) in eq (13a) and rearrangement gives

$$\frac{\dot{\sigma}_f}{\dot{\sigma}_1} = A^{-\frac{\delta(1+\theta)}{\alpha}} C^{-\delta} D \left(\frac{\dot{\epsilon}_n}{\dot{\epsilon}_1}\right)^{\frac{\delta(1+\theta)}{\alpha}} \qquad (17a)$$

which reduces, using Table 1, to

$$\frac{\dot{\sigma}_f}{\dot{\sigma}_1} = 3.3 \times 10^3 \left(\frac{\dot{\epsilon}_n}{\dot{\epsilon}_1}\right)^{1.07} \qquad (17b)$$

Experimental results are compared with eq (17b) in Fig. 12. Except for very slow tests, a continuity in the loading response of the system is evident in all other tests, including premature failures, and strengthens further the concept of using stress rate for the analysis of the experimental data and the response of the system.

Equation (17b) leads to the effective modulus of the system, E_s, given by

$$E_s = \frac{\dot{\sigma}_f}{\dot{\sigma}_1} \Big/ \frac{\dot{\epsilon}_n}{\dot{\epsilon}_1} = 3.3 \times 10^3 \left(\frac{\dot{\epsilon}_n}{\dot{\epsilon}_1}\right)^{0.07} \qquad (18)$$

It is convenient here to introduce the term 'failure modulus', E_f, defined as

$$E_f = \frac{\sigma_f}{\sigma_1} \Big/ \epsilon_f \qquad (19)$$

Substitution of ϵ_f from eq (5a) and σ_f/σ_1 from eq (1a) in eq (19) and rearrangement gives

$$E_f = A^{-\frac{1-\beta+\theta}{\alpha}} B^{-1} C^{-1} \left(\frac{\dot{\epsilon}_n}{\dot{\epsilon}_1}\right)^{\frac{1-\beta+\theta}{\alpha}} \quad (20a)$$

which relates the failure modulus in terms of nominal strain rate. This reduces, on substitution of the values of the constants from Table 1, to

$$E_f = 7.3 \times 10^3 \left(\frac{\dot{\epsilon}_n}{\dot{\epsilon}_1}\right)^{0.08} \quad (20b)$$

Both the eqs (18) and (20b) are nonlinear and show that E_s is smaller than E_f at any $\dot{\epsilon}_n$. This indicates that the total system is softer than the specimen. The E_s value of 1.7 GN • m^{-2} at 1×10^{-4} s^{-1} is considerably lower than the E_f value of 3.5 GN • m^{-2} which, on the other hand, is appreciably lower than the Young's modulus of $\approx$ 9.5 GN • m^{-2} of ice used.[1] Abrupt splitting type of failures at $\dot{\epsilon}_n$ just above 10^{-4} s^{-1} are therefore far from conditions of truly elastic loading and, hence, far from truly brittle behavior.

An explanation as to why the strain rate in the specimen could be different from nominal strain rate is given in Ref. 14 which also discusses our test results on machines and systems of varying stiffness characteristics. It is shown that if there is no change in any of the components in the loading column, including specimen geometry and type of ice, then test machines differing significantly in rigidity could have a marked influence on system stiffness. A stiff machine could result in greater stress rate and therefore greater yield strength at the same $\dot{\epsilon}_n$ than a soft machine, and could shift the occurrence of premature failure to lower strain rate on the $\dot{\epsilon}_n$ scale. Preliminary experiments with two other test machines with 2.5 and 12.5 times greater load capacity than the machine used in this experiment confirmed this hypothesis.[14]

It is shown further that change in any of the system components, for example specimen geometry,[14] or introduction of compliant platens[14] to improve end conditions, affects system stiffness, stress rate and specimen strain rate and, thus, strength at a given $\dot{\epsilon}_n$. Available strength results,[6-11,13] reported as functions of nominal strain rates therefore require reanalysis and reinterpretation. This conclusion is further strengthened by the fact that there is ample evidence in the literature of large discrepancies between nominal strain rates and corresponding strain rates in the specimen. The tabulated results in Ref. 11, for example, show the average strain rates to failure to be 10 to 100 times less than the corresponding nominal strain rates; these discrepancies were not, however, discussed. The deformation characteristics of ice during strength testing can now be described analytically.[15]

Conclusions

A conventional test machine capable of delivering constant displacement rates was used to investigate the uniaxial compressive strength of columnar-grained ice at a constant temperature. Although a definite relation was observed between yield stress, σ_f, and the nominal strain rate, $\dot{\epsilon}_n$, the specimen strain rates were far from constant during the tests and approached $\dot{\epsilon}_n$ only at peak stresses. A strong dependence of failure time, t_f, on σ_f was noted for conditions exhibiting upper yield. $\dot{\epsilon}_n$ in conjunction with t_f, however, overestimated the failure strain, ϵ_f. Better but still not satisfactory representation of the deformation history was obtained by using the average strain rate to yield, $\dot{\epsilon}_{af}$. This allowed an interrelation to be formulated between the various measured quantities. A systematic dependence between σ_f and ϵ_f was shown to exist for upper yield conditions. Specimens that behaved viscously exhibited greater strain than that given by this relation, whereas those that failed abruptly underwent less strain. Analysis showed that the actual loading history comprised a nearly constant stress rate up to about 90 percent of yield stress, followed thereafter by a path leading to a constant strain rate. It was more appropriate, therefore, to treat the tests as occurring at constant stress rate rather than at constant strain rate.

Results were reanalyzed in terms of stress rate. This allowed the effect of machine stiffness to be taken into consideration and a prediction to be made of its possible influence on measured strengths. A stiff machine could result in higher yield strength than a soft one at the same $\dot{\epsilon}_n$ and could shift the occurrence of abrupt failure to lower strain rates. The mode of failure was found to be related to structural deterioration resulting from internal crack formation. Introduction of the concept of a failure modulus for yield type of failures and the formulation of its dependence on nominal strain rate helped to show that the apparently brittle, abrupt failures were not associated with truly elastic loading conditions.

Acknowledgments

The author is indebted to D. Wright for his assistance in designing and conducting the tests, and for performing some tedious measurements. He is also grateful to R. Frederking for allowing the use of results on St. Lawrence River ice, and to M. Nakawo for accurately measuring the density of the ice used.

This paper is a contribution from the Division of Building Research, National Research Council of Canada and is published with the approval of the Director of the Division.

References

1. Sinha, N.K., "Rheology of Columnar-grained Ice," EXPERIMENTAL MECHANICS, **18** *(12), 464-470 (1978).*

2. Sinha, N.K., "Short-term Rheology of Polycrystalline Ice," J. Glaciology, **21** *(85), 457-473 (1978).*

3. Gold, L.W., "The Process of Failure of Columnar-grained Ice," Phil. Mag., **26** *(2), 311-328 (1972).*

4. Sinha, N.K., "Dislocations in Ice as Revealed by Etching," Phil. Mag., **36** *(6), 1385-1404 (1977).*

5. Sinha, N.K., "Observation of Basal Dislocations in Ice by Etching and Replicating," J. Glaciology, **21** *(85), 385-395 (1978).*

6. Gold, L.W. and Krausz, A.S., "Investigation of the Mechanical Properties of St. Lawrence River Ice," Can. Geotech. J., **8** *(2), 163-169 (1971).*

7. Frederking, R., "Plane-strain Compressive Strength of Columnar-grained and Granular-snow Ice," J. Glaciology, **18** *(80), 505-516 (1977).*

8. Ramseier, R.O., "Growth and Mechanical Properties of River and Lake Ice," Ph.D. Thesis, Laval University, Quebec, Canada (1976).

9. Muguruma, J., "Effects of Surface Conditions on the Mechanical Properties of Ice Crystals," J. Phys., D, Ser. 2, **2**, *1517-1525 (1969).*

10. Gold, L.W., "Engineering Properties of Fresh-water Ice," J. Glaciology, **19** *(81), 197-212 (1977).*

11. Hawkes, I. and Mellor, M., "Deformation and Fracture of Ice under Uniaxial Stress," J. Glaciology, **11** *(61), 103-131 (1972).*

12. Frederking, R., Private communication.

13. Haynes, F.D. and Mellor, M., "Measuring the Uniaxial Compressive Strength of Ice," J. Glaciology, **19** *(81), 213-223 (1977).*

14. Sinha, N.K. and Frederking, R.M.W., "Effect of Test System Stiffness on Strength of Ice," Proc. 5th International Conference on Port and Ocean Engineering under Arctic Conditions. Aug. 13-18, Trondheim, Norway; **1**, *708-717 (1979).*

15. Sinha, N.K., "Application of Creep Model of Ice to Predict Its Response During Strength Tests." Presented at Fourth SESA International Congress on Experimental Mechanics, Boston, MA, May 25-30, 1980.